Journal of Alloys and Compounds 509 (2011) 4905–4909

Contents lists available at ScienceDirect

Journal of Alloys and Compounds

journal homepage: www.elsevier.com/locate/jallcom

Microstructure and wear behavior of stellite 6 cladding on 17-4 PH stainless steel

A. Gholipour, M. Shamanian*, F. Ashrafizadeh

Department of Materials Engineering, Isfahan University of Technology, Isfahan 84156-83111, Iran

ARTICLE INFO

Article history:
Received 15 May 2010
Received in revised form
26 September 2010
Accepted 28 September 2010
Available online 23 February 2011

Keywords:
17-4PH stainless steel
Weld overlay
Microstructure
Wear
Stellite 6

ABSTRACT

This paper deals with the investigation of the microstructure and wear behavior of the stellite 6 cladding on precipitation hardening martensitic stainless steel (17-4PH) using gas tungsten arc welding (GTAW) method. 17-4 PH stainless steel is widely used in oil and gas industries. Optical metallography, scanning electron microscopy (SEM) and energy dispersive spectroscopy (EDS) were employed to study the microstructure and wear mechanisms. X-ray diffraction analysis was also used to identify phases formed in the coating. The results showed that the microstructure of the surface layer consisted of carbides embedded in a Co-rich solid solution with a dendritic structure. In addition, the dendritic growth in the coating was epitaxial. Primary phases formed during the process were Co (fcc), Co (hcp), lamellar eutectic phases, $M_{23}C_6$ and Cr_7C_3 type carbides. The results of the wear tests indicated that the delamination was the dominant mechanism. So, it is necessary to apply an inter-layer between the substrate and top coat.

1. Introduction

Stainless steels are widely used in industry since application of such materials leads to increase in service life and reduction of energy consumption [1]. In this regard, precipitation hardened stainless steels with good corrosion resistance, high strength, low distortion, excellent weldability and high hardness (up to 49 HRC), are of considerable interest. Alloy 17-4 PH is the most well known material among the precipitation hardened stainless steels with unique properties which is used in oil, gas and aerospace industries [2–4]. The inner surface of vapor taps made from this steel are always exposed to sequential impacts, high temperature, erosion due to evolved gases and fast (turbulent) flows. A solution to this problem is the application of a wear and corrosion resistant coating [5].

Co-base alloys consisted of wear and corrosion resistant carbides have been considered as candidate materials for surface hardening of 17-4 PH stainless steel. An acceptable wear resistance can be expected when appropriate type and amount of hard phases are present [5]. Stellite, a type of cobalt based superalloy, is extensively used as a surface hardener under harsh conditions of gas turbines and bearings [6–11]. Wear resistance in these alloys is obtained by two mechanisms; formation of carbides in the matrix and solution hardening by the presence of Cr, W, Ta, Nb and Mo. Different features of carbides such as distribution, size and shape are affected by the process conditions. Most of the added elements are carbide formers and their effect on the strength of the solid solution is dependent upon the carbon content [6,12]. Increase in hardness can also be due to formation of intermetallics.

In the related literature, surface alloying is usually done by advanced techniques such as laser cladding due to significant advantages like fast processing speed, relative cleanliness, a very high heating/cooling rate (105 K/s) and high solidification velocity (up to a maximum of 30 m/s) [13]. However, there are practically simpler and more cost-effective methods like gas tungsten arc welding in which by discreet controlling of welding parameters, enhanced surface and wear properties can be achieved [14]. These methods are very effective and are techno-economic solutions to wear problem of materials. The cost of the coated material per unit area may be higher than that of uncoated material, but when it is applied to only critical areas of the components, the increase in the cost may be insignificant regarding to the improvement in performance. In this research, gas tungsten arc welding (GTAW) was used to cladding of 17-4 PH stainless steel with stellite 6. Low price equipments, ability of deposition on complicated shapes with large and small dimensions, and availability of a wide range of materials are advantages of this technique. Although precipitation hardening stainless steels are widely used in industries, but, few papers studied cladding of this type of steel. The aim of the present work was to investigate the surface properties of 17-4 PH alloy cladded with stellite 6.

2. Materials and experimental

17-4 PH stainless steel with the dimensions of 20 mm × 40 mm × 40 mm was used as the substrate material. Stellite 6 alloy in the form of 3 mm diameter wire

* Corresponding author. Tel.: +98 311 3915737; fax: +98 311 3915737.
E-mail address: shamanian@cc.iut.ac.ir (M. Shamanian).

0925-8388/$ – see front matter © 2011 Elsevier B.V. All rights reserved.
doi:10.1016/j.jallcom.2010.09.216

Table 1
Chemical compositions of 17-4PH stainless steel and stellite 6 (wt.%).

	Co	Cr	Si	W	Cu	Mn	Ni	Mo	C	Fe
17-4PH	–	15.8	0.443	–	3.85	0.28	3.77	0.2	<0.1	Bal.
Stellite 6	Bal.	28.87	1	4.31	–	0.49	2.41	<1	1.2	2.95

Table 2
GTAW process parameters.

Electrode	W-2% thorium
Diameter	2.4 mm
Electrode polarity	DCEN
Welding current (A)	160
Welding speed (m/s)	1.3×10^{-3}
Argon, flow rate (L/min)	8

was selected as coating materials. The chemical compositions of stellite and 17-4 PH stainless steel are shown in Table 1.

Gas tungsten arc welding (GTAW) process was used to clad the samples with stellite 6. The GTAW process parameters are provided in Table 2. After cladding, samples were cooled in air and finally subjected to precipitation hardening treatment at 480 °C for 1 h. Microsturctural examinations were carried out using optical microscopy, SEM and EDS. Ferric chloride alcohol reagent used as etchant solution. Pin-on-disc wear tests were used to study the wear properties of the samples. Discs were made from the coated samples and the pin was 52100 bearing steel. Wear tests were conducted in accordance to ASTM G99 and the results were represented in the form of weight loss vs. sliding distance. The friction coefficient was continuously recorded during the test and the worn surfaces were examined by SEM to identify the wear mechanisms.

3. Results and discussion

The dashed line in Co-C phase diagram (Fig. 1) represents the alloy (stellite 6) used in the current study. The first stage of solidification (for stellite 6), by crossing the liquidus, includes solidification of Co solid solution which results in formation of cellular or dentritic. According to Eq. (1), the ratio between G and R is reduced from fusion line (FL) to the center line (CL). Thus, the mode of solidification is changed from planar to cellular, columnar dendrite and equiaxed dendrite throughout the melt zone [15]. Results of optical investigation during different stages of solidification are shown in Fig. 2.

$$\left(\frac{G}{R}\right)_{CL} \ll \left(\frac{G}{R}\right)_{FL} \quad (1)$$

As Co-based solid solution solidifies, melt at inter-dendritic spaces is enriched from carbon and chromium, thus the composition of the melt approaches to the eutectic composition. During the final stages

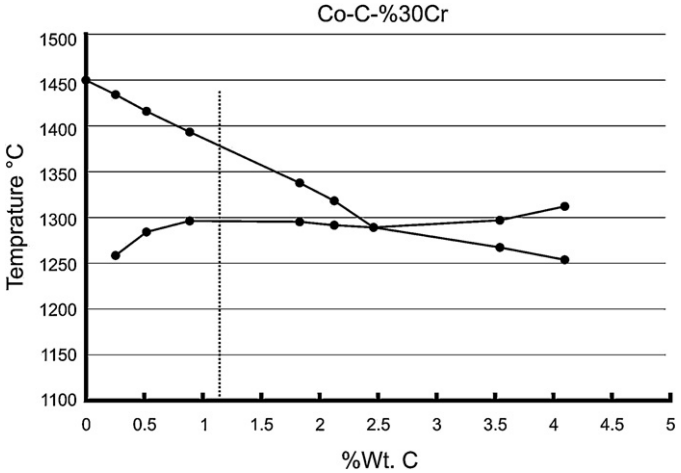

Fig. 1. Phase diagram of stellite 6 used in the current study [20].

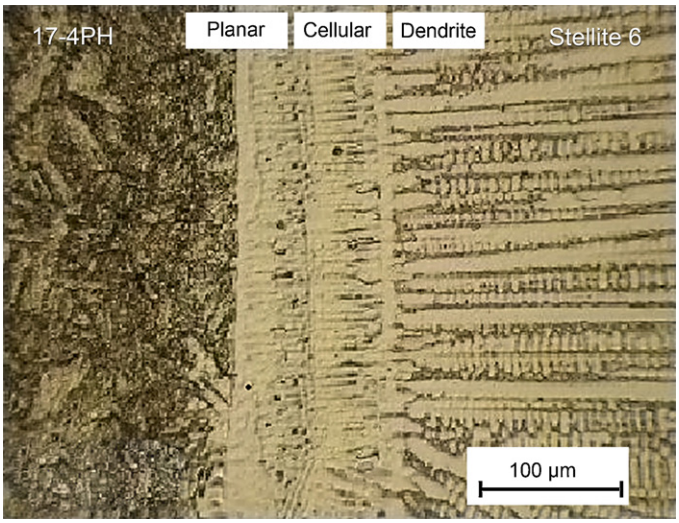

Fig. 2. Optical micrograph showing different stages of solidification.

of the solidification, co-solidification of eutectic solid solution and eutectic $(Cr,Co)_7C_3$ carbides occurs [16].

Results of metallographic micrographs and EDS analysis show that the microstructure consists of Cr-rich matrix (Co-γ phase) and chromium carbide-rich eutectic (Figs. 3 and 4). According to Fig. 4(a), presence of Cr and Fe in the matrix is clear. Since the sensitivity of EDS is too poor to allow the detection of light elements like carbon, so, results are presented regardless of percentage of carbon. The composition of the dark phases consisted of chromium carbides as shown in Fig. 4(b). It is hard to etch the bright areas which have a FCC structure. In contrast, dark areas (less noble phases with HCP structure) can be easily etched [17].

Fig. 5 shows the interface between stellite cladding and 17-4PH stainless steel substrate. As can be seen, the first type of boundary is formed. This type of boundary is likely to have formed in similar metal welding and is different from the second type which generally forms in welding of dissimilar metals. In the second type boundaries, grains grow parallel to the interface of the weld. Grain growth in the first type of boundaries is different. In this condition, grain boundaries form from the boundaries within the base metal

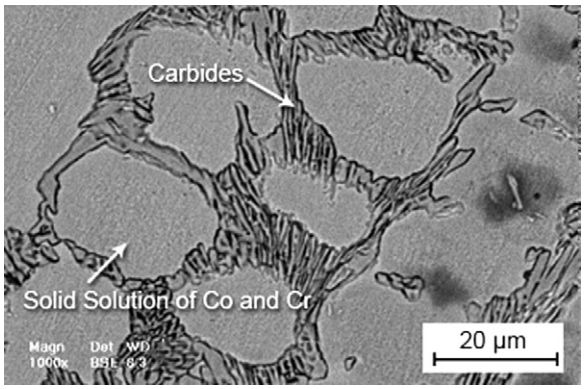

Fig. 3. SEM micrograph of stellite 6 at the middle of the coating.

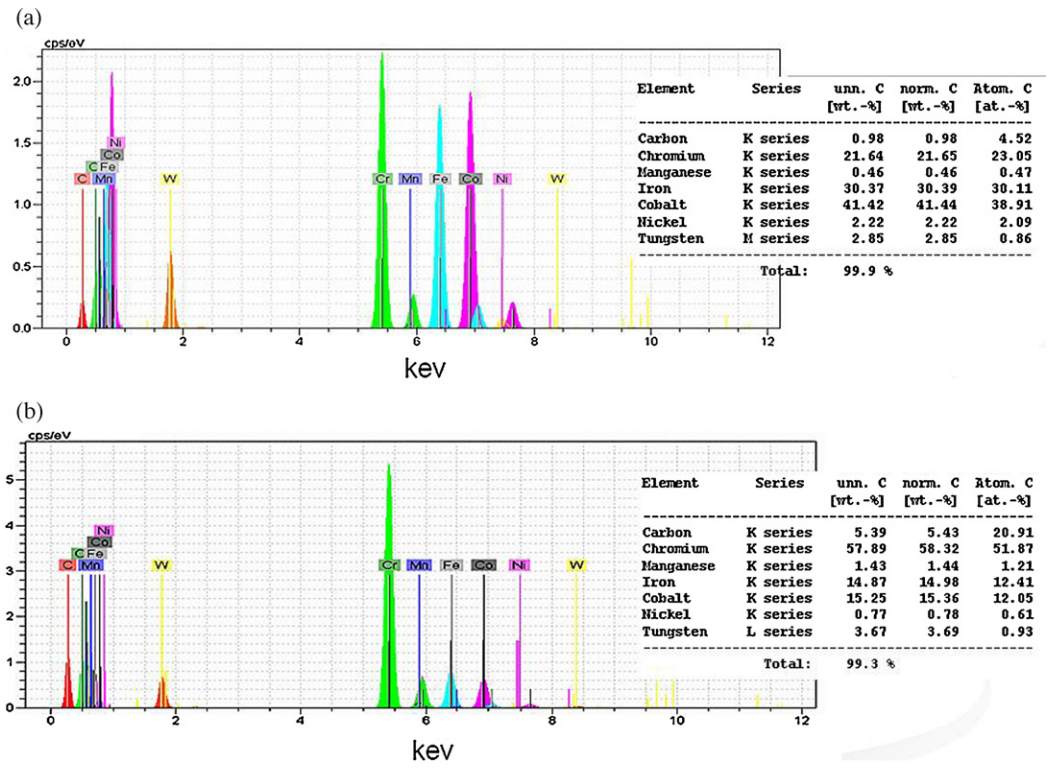

Fig. 4. Results of EDS analysis, (a) bright phase, matrix, (b) dark phase, chromium carbides.

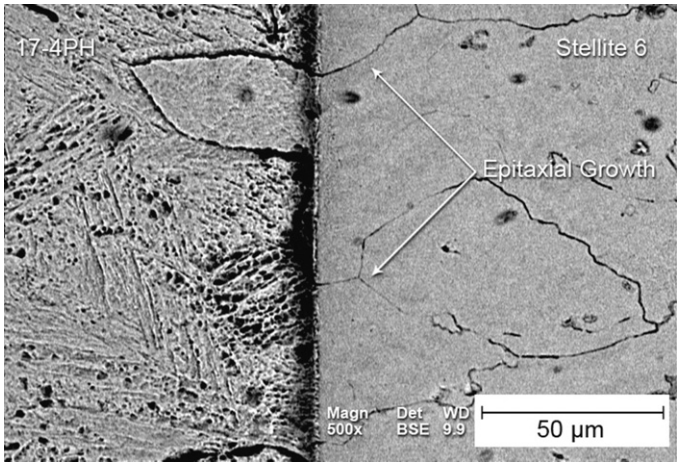

Fig. 5. The interface between stellite cladding and 17-4PH stainless steel substrate.

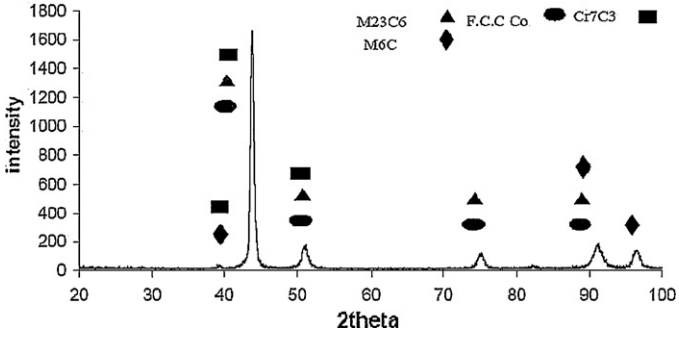

Fig. 6. Phases formed in the stellite 6 coating.

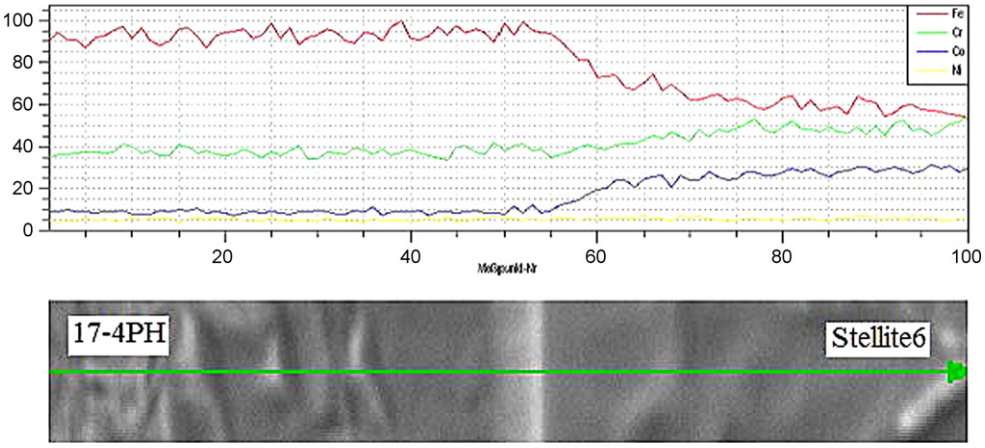

Fig. 7. Line scanning analysis from substrate to coating surface.

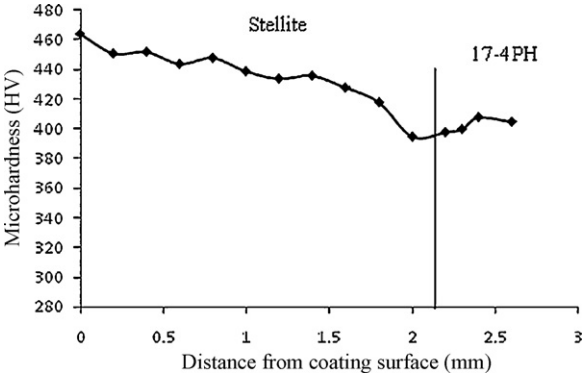

Fig. 8. Microhardness profile from 17-4PH to stellite cladding surface.

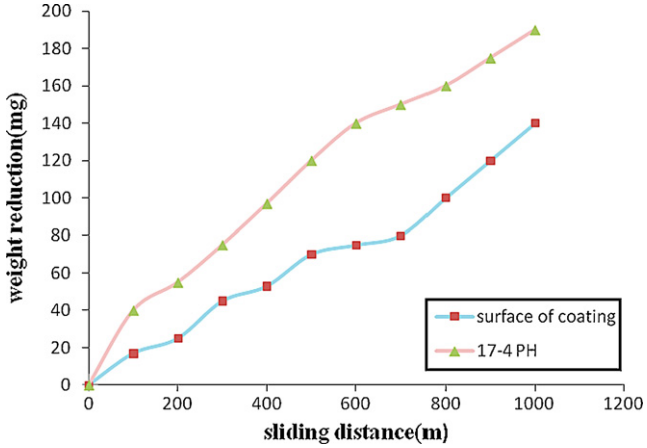

Fig. 9. Weight losses of the cladded specimens.

and then grow in a direction perpendicular to the weld interface into the weld pool. This kind of growth is called epitaxial growth. Similarities in crystal structure and chemical composition result in the evolution of such growth.

Fig. 6 shows the phases formed in the stellite 6 coating at different conditions. As can be seen, the main phase is FCC-Co. Metastable phases such as $Cr_{23}C_6$, Cr_7C_3, M_6C are also present in the XRD patterns.

Line scanning was carried out to investigate dilution of the coating by substrate (Fig. 7). Due to uniform application of cooling rate, the distribution of alloying elements is homogenous in sample. The dilution of stellite by iron causes increased toughness, reduced hardness and corrosion resistance in many corrosive environments [18,19]. It also causes reduced wear resistance because of increase in cobalt lattice stacking fault energy [20]. Therefore, the application of an inter-layer is usually suggested to minimize the dilution [14].

Results of microhardness measurements for bright and dark zones are summarized in Fig. 8. The hardness of carbide-containing zones (dark phases), is higher than that of bright zones. Cr content of dark areas is also higher which results in increase in hardness of these zones. It can be seen that hardness increases from interface to the surface. This is due to the finer size of the grains in comparison to that at interface and also diffusion of Fe adjacent to the interface. Previous studies on microstructure and mechanical properties of stellite 6 showed that increase in the hardness of the weld metal adjacent to the base metal is observed due to formation of a quasi-martensitic structure. Decreases in Co content and increase in Fe content due to the mixing of weld and base metal, cause the instability of HCP structure and formation of martensitic plate with a base centered tetragonal structure [21,22].

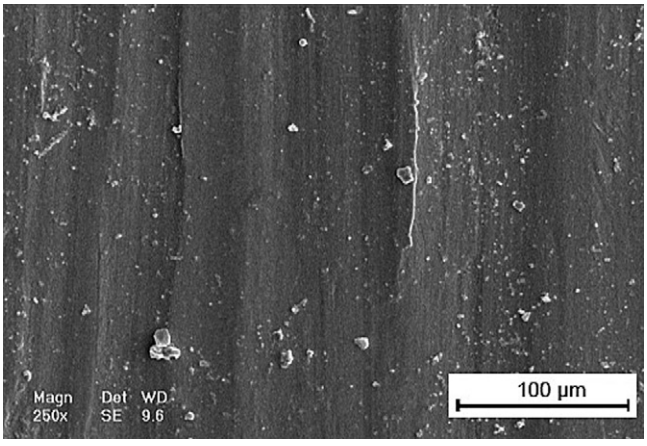

Fig. 10. SEM micrographs of the wear line for the coated sample.

Weigh loss curves versus sliding distance are shown in Fig. 9. It is observed that the values of weight loss of 1-pass stellite 6 sample are lower than that of 17-4PH sample.

Fig. 10 shows the SEM micrographs of the wear line for the coated sample with 1-pass of stellite. As can be seen in this figure, formation of edge and plates as well as plastic deformation of the surface layers is evident. According to the SEM micrographs obtained from the powder products of the wear (Fig. 11(a)), it is seen that the powders are rather coarse. On the other hand, microcracks and voids are evident in the powders (Fig. 11(b)). Plate-like wear debris is consisted of voids and cracks on the surface. When

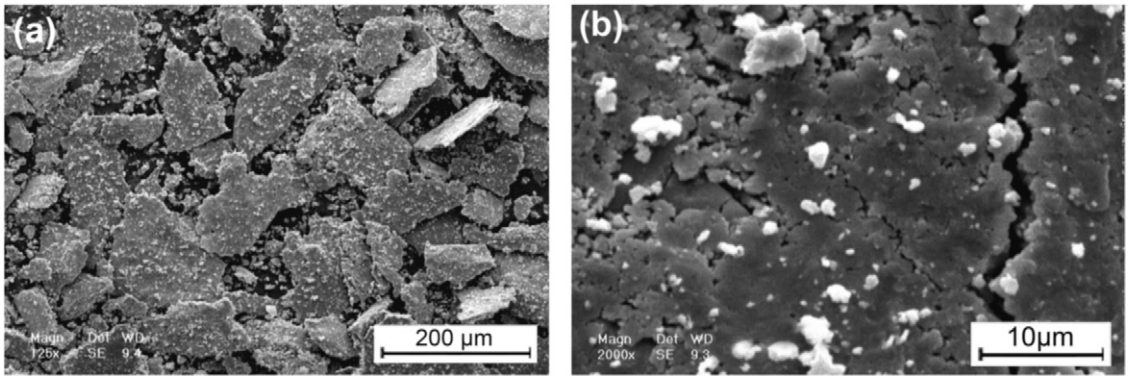

Fig. 11. SEM micrographs obtained from (a) the powder products of the wear and (b) microcracks and voids in the powders.

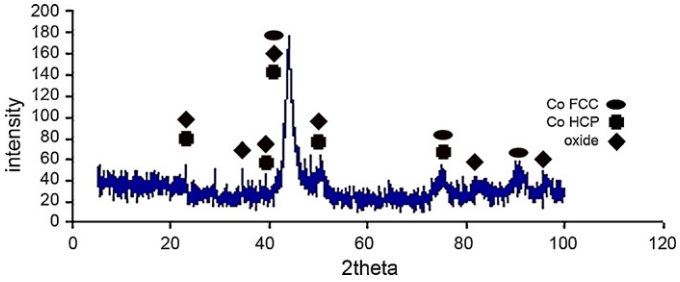

Fig. 12. XRD pattern obtained from the wear debris.

the plate-like wear particles are detached, some of them have curvature while longer ones are serrate. It seems that the delamination is the dominant mechanism of the wear.

Fig. 12 shows the XRD pattern obtained from the resulted powders from the wear sample. Presence of Cr_2O_3 oxide phase is clear in the pattern. It should be mentioned that Cr_2O_3 was not present in the XRD pattern of cladded sample prior to the wear test. Although increase in surface temperature is the main cause of oxide formation, but, oxide particles were also observed even at lower temperatures. It can be envisaged that friction between two surfaces, causes to increase in temperature at the tip of the surface roughness. So, the temperature locally increases and oxide phases are formed [23].

4. Conclusions

In this study stellite 6 coating was applied to 17-4PH stainless steel using GTAW cladding technique. The following conclusions can be drawn from the results obtained:

- The microstructure of the surface layer consisted of carbides embedded in a Co-rich solid solution with dendritic structure. Dendritic growth which occurs in coating is epitaxial. Primary phases formed during the process were identified as Co(FCC) and lamellar eutectic phases ($M_{23}C_6$, M_6C, Cr_7C_3).
- Microhardness profiles showed that hardness increases from interface to the coating surface. This is due to the finer size of the grains at coating surface in comparison to that at interface and also diffusion of Fe adjacent to the interface.
- The delamination was suggested as the dominant mechanism of the wear. In this regard, plate-like wear debris consisted of voids and cracks. In addition, due to increase in surface temperature, Cr_2O_3 oxide phase was formed during wear tests.
- The application of an interlayer was suggested to minimize the dilution in order to improve corrosion resistance and prevent hardness reduction.

References

[1] S. Sun, M. Brandt, J. Harris, Surf. Coat. Technol. 201 (2006) 998–1005.
[2] J.D. Bressan, D.P. Daros, A. Sokolowski, R.A. Mesquita, C.A. Barbosa, J. Mater. Proc. Technol. 205 (2008) 353–359.
[3] S.V. Raj, L.J. Ghosn, B.A. Lerch, M. Hebsur, L.M. Cosgriff, J. Fedo, Mater. Sci. Eng. A 456 (2007) 305–316.
[4] J. Wang, H. Zou, C. Li, S.Y. Qiu, B.L. Shen, Mater. Charact. 57 (2006) 274–280.
[5] R. Ravi Bharath, R. Ramanathan, B. Sundararajan, P. Bala Srinivasan, Mater. Design 29 (2008) 1725–1731.
[6] U. Malayoglu, A. Neville, H. Lovelock, Corros. Sci. 47 (2005) 1911–1931.
[7] T.S. Sidhu, S. Prakash, R.D. Agrawal, Surf. Coat. Technol. 201 (2006) 273–281.
[8] C.D. Opris, R. Liu, M.X. Yao, Mater. Design 28 (2007) 581–591.
[9] B. Singh Sidhu, D. Puri S., J. Mater. Proc. Technol. 159 (2005) 347–355.
[10] M.X. Yao, J.B.C. Wu, W.R. Xu, Mater. Sci. Eng. A 407 (2005) 291–298.
[11] G. Xu, M. Kutsuna, Z. Liu, K. Yamada, Surf. Coat. Technol. 201 (2006) 1138–1144.
[12] J. Chen, X.Y. Li, T. Bell, H. Dong, Wear 264 (2008) 157–165.
[13] J.D. Majumdar, A. Kumar, L. Li, Tribol. Int. 42 (2009) 750–753.
[14] Hardsurfacing Application Manual, A Guide for Selection and Use of Hardfacing Welding.
[15] S. Kou, Welding Metallurgy, John Wiley and Sons, New Jersy, 2003.
[16] F. Maiek, Quality variability in cobalt-base hardfacing alloys, Ph.D. Thesis. Cranfield Institute of Technology (1990).
[17] T. Matkovic, P. Matkovic, J. Malina, J. Alloy Compd. 366 (2004) 293–297.
[18] W.C. Lin, C. Chen, Surf. Coat. Technol. 200 (2006) 4557–4563.
[19] A. Asphahani, Haynes International, "Corrosion of Cobalt-Base Alloys", ASM Metals. Handbook, vol. 13 (1987), 9th, 658–662.
[20] L. Fouilland, M. El Mansori, A. Massaq, J. Mater. Proc. Technol. 209 (2009) 3366–3373.
[21] M.G. Burke, T.G. Hicks, M.W. Phaneuf, Microsc. Microanal. 11 (2005) 2014–2016.
[22] G. Xu, M. Kutsuna, Z. Liu, L. Sun, Surf. Coat. Technol. 201 (2006) 3385–3392.
[23] S. Grainger, Alloy Metal Rev. 10 (1961), No.2.